

# Finding outliers in Gaussian model-based clustering

Katharine M. Clark and Paul D. McNicholas

Department of Mathematics & Statistics, McMaster University, Ontario, Canada.

## Abstract

Clustering, or unsupervised classification, is a task often plagued by outliers. Yet there is a paucity of work on handling outliers in clustering. Outlier identification algorithms tend to fall into three broad categories: outlier inclusion, outlier trimming, and *post hoc* outlier identification methods, with the former two often requiring pre-specification of the number of outliers. The fact that sample squared Mahalanobis distance is beta-distributed is used to derive an approximate distribution for the log-likelihoods of subset finite Gaussian mixture models. An algorithm is then proposed that removes the least plausible points according to the subset log-likelihoods, which are deemed outliers, until the subset log-likelihoods adhere to the reference distribution. This results in a trimming method, called OCLUST, that inherently estimates the number of outliers.

**Keywords:** Clustering; model selection; mixture models; OCLUST; outlier.

## 1 Introduction

Classification aims to partition data into a number of groups, or classes, such that observations in the same group are in some sense similar to one another and different to observations in other groups. Clustering is unsupervised classification, in that none of the group memberships are known *a priori*. Many clustering algorithms originate from one of three major methods: hierarchical clustering,  $k$ -means/medoids clustering, and mixture model-based clustering. Additional popular methods include spectral and density-based clustering. Hierarchical clustering either iteratively merges (agglomerative) or splits (divisive) clusters, while  $k$ -means/medoids aims to minimize distance from each point to its cluster centre. Spectral clustering is based in graph theory, where a similarity matrix is used to map nearby points into a lower dimension. The mapped points are then clustered by distance with traditional algorithms, e.g.,  $k$ -means. Density-based methods, such as DBSCAN (Ester et al., 1996), cluster based on number of points within a certain proximity to other points. Although distance-based clustering remains popular, the mixture modelling approach has become increasingly prevalent due to its robustness and mathematical interpretability (McNicholas, 2016a,b). Typically, in the mixture modelling framework for clustering, each component corresponds to a unique cluster, and a cluster is a sample of points from the component

distribution. Although the model can employ almost any component distribution, Gaussian components have been popular due their tractability. Most mixture model-based clustering methods assume, either explicitly or implicitly, that the data — and the clusters — are free of outliers.

Mixture model-based clustering involves maximizing the likelihood of the mixture model. The density of a  $G$ -component Gaussian mixture model is a convex linear combination of component densities and is given by

$$f(\mathbf{x} \mid \boldsymbol{\vartheta}) = \sum_{g=1}^G \pi_g \phi(\mathbf{x} \mid \boldsymbol{\mu}_g, \boldsymbol{\Sigma}_g), \quad (1)$$

where

$$\phi(\mathbf{x} \mid \boldsymbol{\mu}_g, \boldsymbol{\Sigma}_g) = \frac{1}{\sqrt{(2\pi)^p |\boldsymbol{\Sigma}_g|}} \exp \left\{ -\frac{1}{2} (\mathbf{x} - \boldsymbol{\mu}_g)' \boldsymbol{\Sigma}_g^{-1} (\mathbf{x} - \boldsymbol{\mu}_g) \right\}$$

is the density of a  $p$ -dimensional random variable  $\mathbf{X}$  from a Gaussian distribution with mean  $\boldsymbol{\mu}_g$  and covariance matrix  $\boldsymbol{\Sigma}_g$ ,  $\pi_g > 0$  is the mixing proportion such that  $\sum_{g=1}^G \pi_g = 1$ , and  $\boldsymbol{\vartheta} = \{\pi_1, \dots, \pi_G, \boldsymbol{\mu}_1, \dots, \boldsymbol{\mu}_G, \boldsymbol{\Sigma}_1, \dots, \boldsymbol{\Sigma}_G\}$  denotes the parameters.

An outlier can be considered an observation “that appears to deviate markedly from other members of the sample in which it occurs” (Grubbs, 1969). The two main types of outliers are mild outliers and gross outliers (Ritter, 2014, pp. 79–80). Mild outliers may be near other points in a cluster but they are unusual relative to the distribution of the cluster. Gross outliers are unpredictable and are not modeled by any probability distribution. They do not exist in close proximity to any of the clusters. Outliers may occur due to (unlikely) random chance, or they may arise due to experimental, measurement, or recording error (Grubbs, 1969).

A noisy dataset was simulated by generating three Gaussian clusters and adding uniform noise, and is shown on the left-hand side of Figure 1. The uniform noise can be thought of as representing mostly gross or mild outliers; however, some of the uniform noise overlaps with a cluster and so would be classified as belonging to the cluster by any sensible method. Applying the `mixture` (Pocuca et al., 2024) package for R (R Core Team, 2023) to these data, with  $G = 3$  components, leads to the result depicted on the right-hand side of Figure 1. This solution merges two of the clusters and places some outliers into their own cluster. Therefore, the result of failing to account for outliers is an ill-fitting model which misrepresents the structure of the data.

In general, outliers, particularly gross ones, can significantly impact the parameter estimates. For example, when fitting a mixture model, outliers may draw component means towards them and inflate component covariance matrices. In the case of our simulated example, the originally-spherical clusters are elongated (Figure 1). It is thus beneficial to either remove outliers or reduce their effect by accounting for them. The proposed OCLUST algorithm is designed to handle both mild and gross outliers.

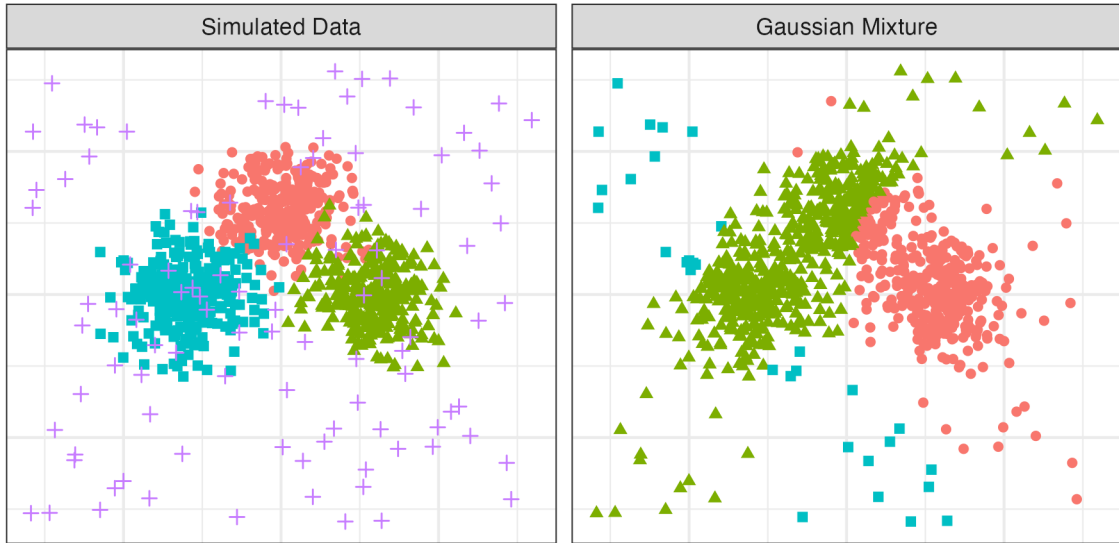


Figure 1: A simulated dataset with three Gaussian clusters and uniform noise. Colours represent the simulated classes (left) and predicted classes using the `mixture` package (right).

## 2 Related Work

### 2.1 Outliers in Unsupervised Gaussian Model-Based Clustering

In Gaussian model-based clustering, outlier methods usually fall into one of three paradigms: outlier inclusion, *post hoc* outlier identification, and outlier trimming. The first method, proposed by [Banfield and Raftery \(1993\)](#), includes outliers in an additional uniform component over the convex hull. If outliers can be treated as cluster-specific and are symmetric about the component means, we can incorporate them into the tails if we cluster using mixtures of multivariate power exponential ([Dang et al., 2015](#)), Pearson type VII ([Sun et al., 2010](#)), multivariate leptokurtic-normal ([Bagnato et al., 2017](#)), multivariate shifted exponential normal, multivariate tail-inflated normal ([Tomarchio et al., 2022](#)), or multivariate t-distributions ([Peel and McLachlan, 2000](#); [Andrews and McNicholas, 2011](#)). [Punzo and McNicholas \(2016\)](#) introduce mixtures of contaminated Gaussian distributions, where each cluster has a proportion  $\alpha_g \in (0.5, 1)$  of ‘good’ points, with density  $\phi(\mathbf{x} \mid \boldsymbol{\mu}_g, \boldsymbol{\Sigma}_g)$ , and a proportion  $1 - \alpha_g$  of ‘bad’ points, with density  $\phi(\mathbf{x} \mid \boldsymbol{\mu}_g, \eta_g \boldsymbol{\Sigma}_g)$ . Within component  $g$ , each distribution has the same mean  $\boldsymbol{\mu}_g$ , but the ‘bad’ points have an inflated covariance matrix  $\eta_g \boldsymbol{\Sigma}_g$ , where  $\eta_g > 1$ .

Instead of fitting outliers in the model, we may wish just to identify outliers after the model has been fit. This is of particular interest in novelty detection. [Evans et al. \(2015\)](#) identify outliers first by fitting a Gaussian mixture model, then quantifying the extent the variance changes when a point is removed. Points that inflate the variance beyond a certain threshold if included are deemed outliers.

Finally, it may be of interest to trim outliers from the dataset. [Cuesta-Albertos et al. \(1997\)](#) developed an impartial trimming approach for  $k$ -means clustering; however, this

method maintains the drawback of  $k$ -means clustering, where the clusters are spherical with equal — or, in practice, similar — radii or they are so well separated that a departure from this shape constraint will not matter. Of course, the latter is a trivial case and is mentioned only for completeness. [García-Escudero et al. \(2008\)](#) improved upon trimmed  $k$ -means with the TCLUS algorithm. TCLUS places a restriction on the eigenvalue ratio of the covariance matrix, as well as implementing a weight on the clusters, allowing for clusters of various elliptical shapes and sizes. [García-Escudero et al. \(2011\)](#) extends TCLUS to Gaussian mixture modelling. An obvious challenge with these methods is that the eigenvalue ratio must also be known *a priori*. There exists an estimation scheme for the proportion of outliers but it is heavily influenced by the choices for number of clusters and eigenvalue ratio. It is of great interest to develop a trimming approach within the model-based clustering domain that does not require pre-specification of the proportion of outliers. This is important because, for most real datasets, the proportion of outliers is *a priori* unknown.

## 2.2 General Unsupervised Outlier Detection Methods

Some traditional approaches to outlier analysis identify points with outlier scores greater than a certain threshold. For example, we can generate a score for each data point using a measure of central tendency  $a$  and a measure of variability  $b$ . Points are considered outliers if their scores are larger than some threshold  $c$ , i.e.,  $|\frac{x-a}{b}| > c$  or  $x \notin (a - bc, a + bc)$ . Examples include the three sigma rule ( $c = 3$ ) and the median absolute difference thresholding strategy ([Hampel, 1974](#)). [Yang et al. \(2019\)](#) make this method robust by applying the thresholding procedure twice, while [Buzzi-Ferraris and Manenti \(2011\)](#) remove outliers one-by-one by iteratively applying a clever mean threshold.

In the clustering framework, similar outlier scores can be generated using the distance to the cluster centre ([Hautamäki et al., 2005](#)) or to the nearest neighbours ([Ramaswamy et al., 2000](#)). We can also consider points of low density to be outliers, for example in [Knorr and Ng \(1998\)](#), where points with few neighbours within a specified distance are identified, or DBSCAN, which clusters data based on density, with points not placed in clusters classified as noise. [Fränti and Yang \(2018\)](#) smooth noisy data by replacing each point by the mean of its nearest neighbours. They repeat this process several times to obtain better centroid locations and  $k$ -means classification. [Yang et al. \(2021\)](#) take this one step further by treating the distance each point is shifted as an outlier score.

[Boukerche et al. \(2020\)](#) provide a detailed survey of methods to address outliers in unsupervised classification. They include approaches which are proximity- or projection-based, and techniques for high-dimensional, streaming, or ‘big’ data. While these methods could be used to identify observations that deviate from the entire dataset, some cannot consider points which are spurious in relation to the cluster structure. Although [Boukerche et al. \(2020\)](#) include cluster-based approaches, the methods they consider typically concern groups of outliers which form their own cluster.

## 3 Methodology

### 3.1 Distribution of Subset Log-Likelihoods

In this section, the distribution of squared Mahalanobis distance is used to derive the distribution of subset log-likelihoods, which forms the basis for the proposed OCLUST algorithm. We consider a subset log-likelihood to be the log-likelihood of a model fitted with  $n - 1$  of the data points. Formally, if we denote our complete dataset as  $\mathcal{X} = \{\mathbf{x}_1, \dots, \mathbf{x}_n\}$ , then we can define the  $j$ th subset as the complete dataset with the  $j$ th point removed,  $\mathcal{X} \setminus \mathbf{x}_j = \{\mathbf{x}_1, \dots, \mathbf{x}_{j-1}, \mathbf{x}_{j+1}, \dots, \mathbf{x}_n\}$ . There are  $n$  such subsets.

Consider a dataset  $\mathcal{X} = \{\mathbf{x}_1, \dots, \mathbf{x}_n\}$  in  $p$ -dimensional Euclidian space  $\mathbb{R}^p$ , where each  $\mathbf{x}_i \in \mathcal{X}$  has Gaussian mixture model density  $f(\mathbf{x}_i | \boldsymbol{\vartheta})$  as in (1). The log-likelihood of i.i.d. dataset  $\mathcal{X}$  under the Gaussian mixture model is

$$\ell_{\mathcal{X}}(\boldsymbol{\vartheta}) = \sum_{i=1}^n \log \left[ \sum_{g=1}^G \pi_g \phi(\mathbf{x}_i | \boldsymbol{\mu}_g, \boldsymbol{\Sigma}_g) \right], \quad (2)$$

which we will denote as  $\ell_{\mathcal{X}}$  for simplicity. From (2), the log-likelihood of the model can be expressed as the sum of the logarithm of each point’s probability density. Points near the tails — corresponding to probability density values close to zero — will have a smaller contribution to the log-likelihood than points with higher probability density such as points near the centre of the distribution. Intuitively, the larger the difference in log-likelihood between the subset and full models, the more outlying the point is, i.e., the model improved the most in its absence.

By this logic, we treat the point whose absence produced the largest subset log-likelihood,  $\mathbf{x}_k$  say, as our candidate outlier. Formally, we can express this as follows.

**Definition 1** (Candidate Outlier). *We define our candidate outlier as  $\mathbf{x}_k$ , where*

$$k = \arg \max_{j \in [1, n]} \ell_{\mathcal{X} \setminus \mathbf{x}_j},$$

and  $\ell_{\mathcal{X} \setminus \mathbf{x}_j}$  is the log-likelihood of the subset with the point  $\mathbf{x}_j$  removed.

We continue removing candidate outliers until we obtain our best model, which is determined by the distribution of our subset log-likelihoods, derived below. Note that a random variable  $W$  from a beta distribution has density

$$f_{\text{beta}}(w | \alpha, \beta) = \frac{\Gamma(\alpha + \beta)}{\Gamma(\alpha)\Gamma(\beta)} w^{\alpha-1} (1 - w)^{\beta-1}, \quad (3)$$

where  $0 < w < 1, \alpha > 0, \beta > 0$ .

The derivation requires the complete-data log-likelihood as an approximation of the log-likelihood. Herein, the complete-data comprise the data  $\mathbf{x}_1, \dots, \mathbf{x}_n$  and their cluster memberships  $\mathbf{z}_1, \dots, \mathbf{z}_n$ , where  $\mathbf{z}_i = (z_{i1}, \dots, z_{iG})'$ ,  $z_{ig} = 1$  if  $\mathbf{x}_i$  belongs to the  $g$ th cluster, and  $z_{ig} = 0$  otherwise. In (2), each cluster contributes to the density of every point. Instead,

consider the case where the clusters are well-separated. We can use the complete-data log-likelihood, herein denoted  $l_{\mathcal{X}}$ , which considers only the density of the component to which the point belongs. We formalize this result in Lemma 1, but first we must make the following assumption.

**Assumption 1.** *The clusters are non-overlapping and well separated.*

In practice, Assumption 1 may be relaxed. For more information on the effect of cluster separation, see Appendix A.

**Lemma 1.** *As the separation between the clusters increases,  $l_{\mathcal{X}} \rightarrow l_{\mathcal{X}}$ . In other words, the log-likelihood in (2) converges to  $l_{\mathcal{X}}$ , where*

$$l_{\mathcal{X}} = \sum_{i=1}^n \sum_{g=1}^G z_{ig} \left[ \log \pi_g + \log \phi(\mathbf{x}_i \mid \boldsymbol{\mu}_g, \boldsymbol{\Sigma}_g) \right]. \quad (4)$$

A proof of Lemma 1 may be found in Appendix B. We will maintain Assumption 1 throughout this paper. The quantity  $l_{\mathcal{X}}$  denotes the complete-data log-likelihood for the entire dataset  $\mathcal{X}$ , and we use  $l_{\mathcal{X} \setminus \mathbf{x}_j}$  to denote the complete-data log-likelihood for the  $j$ th subset  $\mathcal{X} \setminus \mathbf{x}_j$ . Finally, we define the variable  $Y_j = l_{\mathcal{X} \setminus \mathbf{x}_j} - l_{\mathcal{X}}$  as the difference between the  $j$ th subset complete-data log-likelihood and the complete-data log-likelihood for the entire dataset. This leads to our main result, which follows as Theorem 1.

**Theorem 1.** *For a point  $\mathbf{x}_j$  belonging to the  $h$ th cluster, i.e.,  $z_{jh} = 1$ , if  $l_{\mathcal{X}}$  is the complete-data log-likelihood and  $Y_j = l_{\mathcal{X} \setminus \mathbf{x}_j} - l_{\mathcal{X}}$ , then  $Y_j \mid (z_{jh} = 1)$  has an approximate shifted and scaled beta density, i.e.,*

$$Y_j \mid (z_{jh} = 1) \sim f_{\text{beta}} \left( \frac{2n_h}{(n_h - 1)^2} (y_j - c) \mid \frac{p}{2}, \frac{n_h - p - 1}{2} \right) \quad (5)$$

for  $c < y_j < \frac{(n_h - 1)^2}{2n_h} + c$ ,  $n_h > p + 1$ , where  $c = -\log \hat{\pi}_h + \frac{p}{2} \log(2\pi) + \frac{1}{2} \log |\mathbf{S}_h|$ ,  $n_h$  is the number of points in cluster  $h$ ,  $\hat{\pi}_h = n_h/n$ ,

$$\mathbf{S}_h = \frac{1}{n_h - 1} \sum_{i=1}^n z_{ih} (\mathbf{x}_i - \bar{\mathbf{x}}_h) (\mathbf{x}_i - \bar{\mathbf{x}}_h)'$$

is the sample covariance matrix of cluster  $h$ , and  $\bar{\mathbf{x}}_h = \frac{1}{n_h} \sum_{i=1}^n z_{ih} \mathbf{x}_i$ .

*Proof.* Our parameters are unknown in unsupervised classification, so we must estimate them. Due to their desirable qualities, we will replace  $\pi_g$ ,  $\boldsymbol{\mu}_g$  and  $\boldsymbol{\Sigma}_g$  by their unbiased estimates:

$$\hat{\pi}_g = n_g/n, \quad \hat{\boldsymbol{\mu}}_g = \bar{\mathbf{x}}_g, \quad \hat{\boldsymbol{\Sigma}}_g = \mathbf{S}_g, \quad (6)$$

where  $n_g = \sum_{i=1}^n z_{ig}$  is the number of observations in the  $g$ th cluster,  $\hat{\pi}_g$  is the sample proportion,  $\bar{\mathbf{x}}_g$  is the sample mean, and  $\mathbf{S}_g$  is the sample covariance for the  $g$ th cluster

considering all observations in the entire dataset  $\mathcal{X}$ . Now consider  $\hat{\pi}_{g \setminus j}$ ,  $\bar{\mathbf{x}}_{g \setminus j}$  and  $\mathbf{S}_{g \setminus j}$ , the sample proportion, sample mean, and sample covariance matrix, respectively, for the  $g$ th cluster considering only observations in the  $j$ th subset  $\mathcal{X} \setminus \mathbf{x}_j$ . We will require  $\hat{\pi}_{g \setminus j} \approx \hat{\pi}_g$ ,  $\bar{\mathbf{x}}_{g \setminus j} \approx \bar{\mathbf{x}}_g$  and  $\mathbf{S}_{g \setminus j} \approx \mathbf{S}_g$  for all  $j$ . Because we have  $\hat{\pi}_{g \setminus j} \rightarrow \hat{\pi}_g$ ,  $\bar{\mathbf{x}}_{g \setminus j} \rightarrow \bar{\mathbf{x}}_g$  and  $\mathbf{S}_{g \setminus j} \rightarrow \mathbf{S}_g$  as  $n_g \rightarrow \infty$  (proof in Appendix B.2), we need the following assumption.

**Assumption 2.** *The number of observations in each cluster,  $n_g$ , is large.*

When  $n_g$  is large, sample parameter estimates  $\hat{\pi}_g$ ,  $\bar{\mathbf{x}}_g$ , and  $\mathbf{S}_g$ ,  $g \in [1, G]$ , approach the true parameters and they are treated as constant for each subset  $\mathcal{X} \setminus \mathbf{x}_j$ ,  $j \in [1, n]$ . Thus, the complete-data log-likelihood for the  $j$ th subset,  $\mathcal{X} \setminus \mathbf{x}_j$ , when  $z_{jh} = 1$  is

$$l_{\mathcal{X} \setminus \mathbf{x}_j} \approx l_{\mathcal{X}} - \log \hat{\pi}_h - \log \phi(\mathbf{x}_j \mid \bar{\mathbf{x}}_h, \mathbf{S}_h). \quad (7)$$

Rearranging (7) yields

$$l_{\mathcal{X} \setminus \mathbf{x}_j} - l_{\mathcal{X}} \approx -\log \hat{\pi}_h + \frac{p}{2} \log(2\pi) + \frac{1}{2} \log |\mathbf{S}_h| + \frac{1}{2} t_j, \quad (8)$$

where  $t_j = (\mathbf{x}_j - \bar{\mathbf{x}}_h)' \mathbf{S}_h^{-1} (\mathbf{x}_j - \bar{\mathbf{x}}_h)$  is the squared Mahalanobis distance for point  $\mathbf{x}_j$  using the sample parameter estimates in (6) when  $z_{jh} = 1$ .

**Lemma 2.** *Sample squared Mahalanobis distance is distributed according to a scaled beta distribution (Gnanadesikan and Kettenring, 1972). When the data are multivariate normally distributed, i.e.,  $\mathbf{X} \sim \text{MVN}(\boldsymbol{\mu}, \boldsymbol{\Sigma})$ ,*

$$\frac{n}{(n-1)^2} T_j \sim f_{\text{beta}} \left( \frac{n}{(n-1)^2} t_j \mid \frac{p}{2}, \frac{n-p-1}{2} \right)$$

for  $0 \leq t_j \leq (n-1)^2/n$ .

Ververidis and Kotropoulos (2008) prove Lemma 2 for all  $n, p$  satisfying  $p < n < \infty$ .

Finally, we will perform a change of variables to prove our main result from Theorem 1. Let  $W_j = \frac{n_h}{(n_h-1)^2} T_j$  and  $Y_j \mid (z_{jh} = 1) = \frac{1}{2} T_j + c$ , where  $c = -\log \hat{\pi}_h + \frac{p}{2} \log(2\pi) + \frac{1}{2} \log |\mathbf{S}_h|$ . Then

$$Y_j \mid (z_{jh} = 1) = \frac{(n_h - 1)^2}{2n_h} W_j + c.$$

Because  $W_j$  is beta distributed, it has density of the form (3). The change of variables allows the density of  $Y_j \mid (z_{jh} = 1)$  to be written

$$f_{Y \mid (z_{jh}=1)}(y_j) = \frac{2n_h}{(n_h-1)^2} \frac{\Gamma(\alpha + \beta)}{\Gamma(\alpha)\Gamma(\beta)} \left[ \frac{2n_h}{(n_h-1)^2} (y_j - c) \right]^{\alpha-1} \left[ 1 - \frac{2n_h}{(n_h-1)^2} (y_j - c) \right]^{\beta-1}, \quad (9)$$

for  $c < y_j < \frac{(n_h-1)^2}{2n_h} + c$ ,  $\alpha > 0$ ,  $\beta > 0$ . Thus,  $Y_j \mid (z_{jh} = 1)$  is distributed according to a shifted and scaled beta distribution, i.e.,

$$Y_j \mid (z_{jh} = 1) \sim f_{\text{beta}} \left( \frac{2n_h}{(n_h-1)^2} (y_j - c) \mid \frac{p}{2}, \frac{n_h - p - 1}{2} \right). \quad (10)$$

□

Now, the density for  $Y_j$  is conditional on  $z_{jh}$ . Denote this density by  $f_h(y)$ . Because  $P(z_{jh} = 1) = \pi_h$  for all  $j$ , the density of  $Y$ , unconditional on  $\mathbf{z}$  is

$$f(y | \boldsymbol{\vartheta}) = \sum_{g=1}^G \pi_g f_g(y | \boldsymbol{\theta}_g), \quad (11)$$

where  $f_g(y | \boldsymbol{\theta}_g)$  is a shifted and scaled beta density described in (9), and  $\boldsymbol{\theta}_g = \{n_g, p, \hat{\pi}_g, \bar{\mathbf{x}}_g, \mathbf{S}_g\}$ .

**Remark 1.** *It is important to note that (11) does not depend on the choice of  $\mathbf{x}_j$ . Rather, it is the distribution for  $n-1$  of the points with any one point  $\mathbf{x}_j$  removed. The random variable  $Y$  has density  $f(y | \boldsymbol{\vartheta})$  from (11) when the data arise from a finite Gaussian mixture model without outliers. Divergence from this distribution indicates a misspecified model, which we assume to be due to the presence of outliers. This forms the basis for the OCLUST algorithm.*

## 3.2 OCLUST Algorithm

Consider  $y_1, \dots, y_n$  to be realizations of the random variable  $Y$ , which has density given by (11). We propose testing the adherence of  $y_1, \dots, y_n$  to the reference distribution in (11) as a way to test for the presence of outliers. In other words, if  $y_1, \dots, y_n$  does not have a beta mixture distribution, then we assume outliers are present in the model. Because  $\ell_{\mathcal{X}}$  converges to  $l_{\mathcal{X}}$  and acts as a good approximation, we will use  $\ell_{\mathcal{X}}$ . This is important because we will need  $\ell_{\mathcal{X} \setminus \mathbf{x}_j}$  for outlier identification and, additionally, it is outputted by many existing clustering algorithms. The algorithm described below uses the log-likelihood and parameter estimates calculated using the expectation-maximization (EM) algorithm (Dempster et al., 1977) for Gaussian model-based clustering; however, other methods may be used for parameter estimation.

The proposed algorithm is called OCLUST. It both identifies likely outliers and estimates the proportion of outliers within the dataset. When  $\mathbf{X}$  is distributed according to a Gaussian mixture model, then  $Y$  has the probability density in (11). If  $y_1, \dots, y_n$  does not come from (11), then  $\mathbf{x}_1, \dots, \mathbf{x}_n$  does not arise from a Gaussian mixture model (1), implying that the model is misspecified. We assume the misspecification is due to outliers. The OCLUST algorithm assumes that the model is otherwise correctly specified and when  $Y$  does not follow the distribution in (11), then outliers are present. The ‘closeness’ of the distribution of  $Y$  to (11) is assessed using the Kullback-Leibler (KL) divergence, estimated via relative frequencies. The algorithm (Algorithm 1) involves removing candidate outliers one-by-one until KL divergence is minimized. At each step, we obtain the log-likelihood of the entire dataset and the log-likelihoods of the  $n$  subsets. We then assess the distribution of subset log-likelihoods and determine our next candidate outlier,  $t$ , according to Definition 1. This candidate outlier is then trimmed and the algorithm continues to the next iteration. Notably, KL divergence generally decreases as outliers are removed and the model improves. Once all outliers are removed, KL divergence increases again as points are removed from the tails. We select the number of outliers as the location of the minimum KL divergence.

The OCLUST algorithm is outlined in Algorithm 1, with  $n$  being the size of the dataset,  $G$  the number of clusters,  $B \in [0, F - 1]$  the number of initially rejected outliers (see Remark 2), and  $F$  the chosen upper bound (see Remark 3). An R implementation of the algorithm is available as the `oclust` package on CRAN (Clark and McNicholas, 2022).

**Remark 2** (Initialization). *In practice, we do not need to start the algorithm with the entire dataset. We may first remove obvious, gross outliers and start the algorithm from this intermediate solution. This greatly reduces computation time by reducing the number of iterations and it may improve classification by decreasing the likelihood of gross outliers being placed into their own clusters.*

**Remark 3** (Choice of  $F$ ). *We choose  $F$  as an upper bound for the number of outliers. It is used to limit the number of iterations for the algorithm to reduce the computation time.  $F$  may be chosen using prior knowledge about the type of data, or we may choose large  $F$  to be conservative. In the absence of any information about the dataset, we could choose, e.g.,  $F = n/4$ , setting the maximum proportion of outliers to be 25%.*

### 3.3 Computational Complexity

Clustering must be performed  $n + 1$  times for each of the  $F + 1$  iterations of the algorithm. In our simulation study, we use the `mixture` package to implement the EM algorithm, the order of which is generally  $O(Gp^3n)$ . As a result, OCLUST is  $O(FGp^3n^2)$ . The computation time can be reduced by initializing the subset models with the parameters from the full model to vastly decrease the number of iterations required within the clustering algorithm. In addition, subset models are independent and can easily be computed in parallel. Computation times for applying OCLUST to the datasets in Section 4 are available in Appendix C. These times are similar to or somewhat faster than the mean-shift outlier detection algorithm when OCLUST is run in parallel. It is important to note that these times for OCLUST take into account the algorithm running to the upper bound  $F$ , which is often unnecessary. Thus, we propose an early stopping criterion below.

The original version of the OCLUST algorithm involves calculating the KL divergence over a range of possible numbers of outliers. The best model is then chosen as the one which minimizes the KL divergence. Instead, consider a stopping rule for the algorithm to minimize the number of iterations required. We can stop the algorithm once the data fit well to the distribution. One way to do this is using Kuiper’s Test (Kuiper, 1960), where

$H_0$  : The data arise from the specified distribution.

$H_A$  : The data contradict the specified distribution.

By conducting Kuiper’s test, we compare the empirical cumulative distribution function (CDF) to the CDF of the proposed beta mixture distribution. The test statistic is of the form

$$T_0 = D^+ + D^-,$$

---

**Algorithm 1** OCLUST algorithm

---

```
1: procedure OCLUST( $\mathcal{X}, n, G, F$ )
2:   (Optional) Identify gross outliers,  $b$ , using method of choice.  $B = \#b$ .
3:   Update:
       $n \leftarrow n - B$ 
       $\mathcal{X} \leftarrow \mathcal{X} \setminus b$ 
4:   for  $f$  in  $B : F$  do
5:     Cluster the data  $\mathcal{X}$  into  $G$  clusters, using a Gaussian model-based
      clustering algorithm, e.g., the EM algorithm in the mixture package
6:     Output  $\ell_{\mathcal{X}}$ , and for each cluster save:  $\mathbf{S}_g, n_g, \hat{\pi}_g$ .
7:     for  $j$  in  $1 : n$  do
8:       Cluster the subset  $\mathcal{X} \setminus \mathbf{x}_j$  into  $G$  clusters, using the method chosen
      in Step 5.
9:       Output  $\ell_{\mathcal{X} \setminus \mathbf{x}_j}$  and calculate  $y_j = \ell_{\mathcal{X} \setminus \mathbf{x}_j} - \ell_{\mathcal{X}}$ .
10:    end for
11:    Generate the density of  $Y$  using (11) and the parameters from Step 6.
12:    Calculate the approximate KL divergence of  $y_1, \dots, y_n$  to the density
      in Step 11, using relative frequencies.
13:    Determine the most likely outlier  $t$  as per Definition 1.
14:    Update:
       $n \leftarrow n - 1$ 
       $\mathcal{X} \leftarrow \mathcal{X} \setminus t$ 
15:  end for
16:  Choose  $f$  for which the KL divergence is minimized
  ▷ This is the predicted number of outliers.
  ▷ Use the model corresponding to iteration  $f$ 
17: end procedure
```

---

where  $D^+ = \max[F_E(y_i) - F_0(y_i)]$  and  $D^- = \max[F_0(y_i) - F_E(y_i)]$ , for  $i \in [1, n]$ ,  $F_0(y_i)$  is the CDF of  $Y$  at point  $y_i$ , and  $F_E(y)$  is the empirical CDF at point  $y_i$  for a sample of size  $n$ , i.e.,  $F_E(y_i) = i/n$ . An approximate p-value can be estimated using Monte Carlo simulation from the proposed distribution in (11). A total of  $m$  datasets of size  $n$  are simulated and the test statistic is calculated for each one. Then, we estimate the p-value as  $(r + 1)/(m + 1)$ , where  $m$  is the number of samples generated and  $r$  is the number of samples to produce a test statistic greater than or equal to  $T_0$  (North et al., 2002). Instead of using KL divergence in the OCLUST algorithm, we calculate the approximate p-value for each iteration and stop once it is higher than a pre-specified significance level, e.g., 5% or 10%.

## 4 Applications

### 4.1 Illustrative Example

To illustrate how the OCLUST algorithm works, we return to the dataset in Figure 1, but add three uniform outliers instead of 100. We run the OCLUST algorithm using the `oclust` package (Clark and McNicholas, 2022), setting  $B = 0$  and  $F = 10$ . We achieve minimum KL divergence after the three outliers are removed. The optimal solution and corresponding KL graph are plotted in Figure 2.

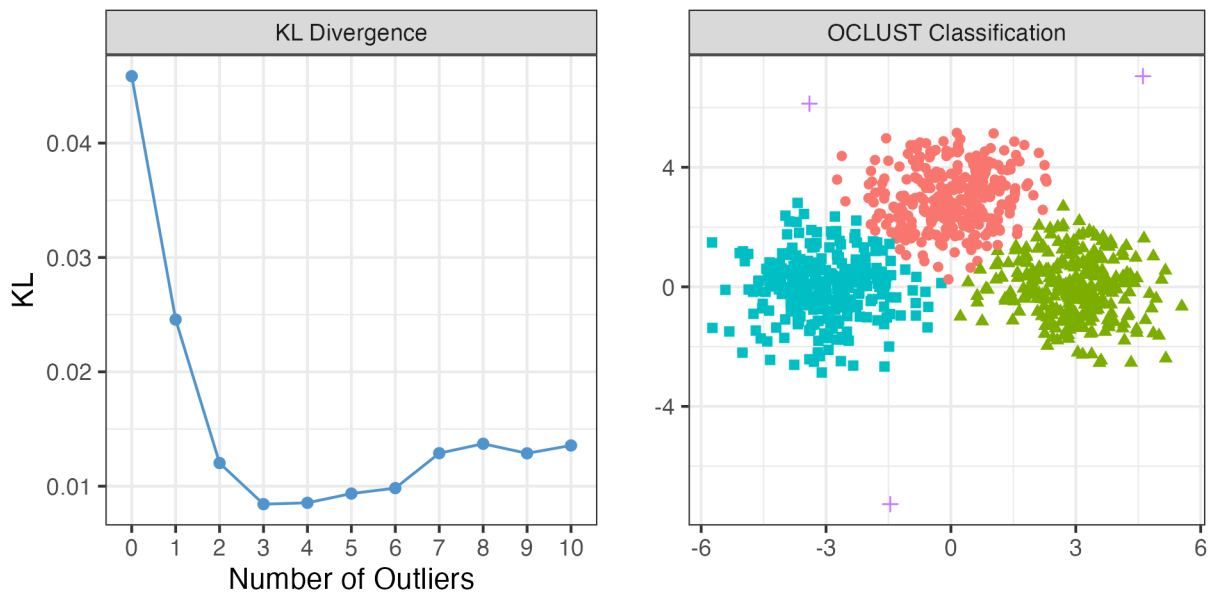


Figure 2: Results from the illustrative example in Section 4.1, with a graph of KL divergence (left) and predicted classifications by the OCLUST algorithm (right).

### 4.2 Simulation Study

The following simulation study tests the performance of OCLUST against the following five popular algorithms:

- Contaminated normal mixtures (CNMix; Punzo and McNicholas, 2016);
- Noise component mixtures — mixtures of Gaussian clusters and a uniform component (NCM; Banfield and Raftery, 1993);
- DBSCAN;
- Mean-shift outlier detection and filtering (Fränti and Yang, 2018); and
- 2T (Yang et al., 2019), i.e., a thresholding approach.

OCLUST is a trimming method which removes outliers from the model. In contrast, CNMix and NCM are outlier inclusion methods. CNMix treats outliers as contamination and assumes the outliers are cluster-specific and reside around the clusters. NCM assumes that outliers are included uniformly. DBSCAN treats clusters as density-connected points and outliers as points that do not belong to clusters. Mean-shift outlier detection is a pre-processing step for a subsequent clustering algorithm. Finally, the thresholding approach considers a point an outlier if the outlier ‘score’ exceeds a specified threshold. Following Yang et al. (2019), we apply this procedure twice (2T). Calculated before clustering, we choose the outlier ‘score’ to be the squared Mahalanobis distance from the centre of the dataset. This measure accounts for differences in variability among dimensions. Subsequently, we cluster the remaining data using the EM algorithm in the `mixture` package. These methods are broadly classified into two types: those that remove outliers and then cluster (mean-shift and 2T) and those that do both simultaneously (OCLUST, CNMix, NCM, DBSCAN).

The following simulation scheme closely follows that in Fränti and Yang (2018). We use the same eight two-dimensional benchmark datasets plus one 32-dimensional dataset (Fränti and Sieranoja, 2018). Sets S1–S4 investigate increasing degrees of overlap. There is a mix of 15 spherical and non-spherical Gaussian clusters with overlap ranging from 9% to 44%. Sets A1–A3 have increasing numbers of clusters, with all sets having spherical Gaussian clusters with equal cluster sizes, deviation, and overlap. The Unbalance set has three clusters densely populated with 2000 points each and five clusters sparsely populated with 100 points each. The Dim032 dataset has 16 well-separated Gaussian clusters in 32 dimensions. The datasets are summarized in Table 1 and plotted in Figure 3, with a two-dimensional projection shown for the Dim032 dataset.

Table 1: Datasets used in the simulation study, where U and D32 represent the Unbalance and Dim032 sets, respectively, and  $F$  indicates the upper bound used in the OCLUST algorithm.

Dataset	A1	A2	A3	S1	S2	S3	S4	U	D32
Size	3000	5250	7500	5000	5000	5000	5000	6500	1024
Clusters	20	35	50	15	15	15	15	8	16
Noise	210	368	525	350	350	350	350	455	72
$F$	300	525	750	500	500	500	500	650	110

Following Fränti and Yang (2018), we set the proportion of outliers at 7%. We generate uniform noise in each dimension in the range  $[x_{\text{mean}} - 2 \times \text{range}, x_{\text{mean}} + 2 \times \text{range}]$ , where the range is the difference between the farthest observation and the mean in each dimension.

We run `oclust` in R, fixing the upper bound  $F$  from Table 1, i.e., at or about 10% of the original data size. We eliminate initial gross outliers with large squared Mahalanobis distances to regions of high density identified by the `dbscan` package (Hahsler et al., 2019). Covariance matrices for the S sets, A sets, and Unbalance set are unrestricted, allowing varying volumes, shapes, and orientations among the clusters. We restrict the Dim032 set to a variance structure with varying volumes and spherical shapes to hasten computation time. We run CNMix using the `CNmixt` function from the `ContaminatedMixt` package (Punzo et al.,

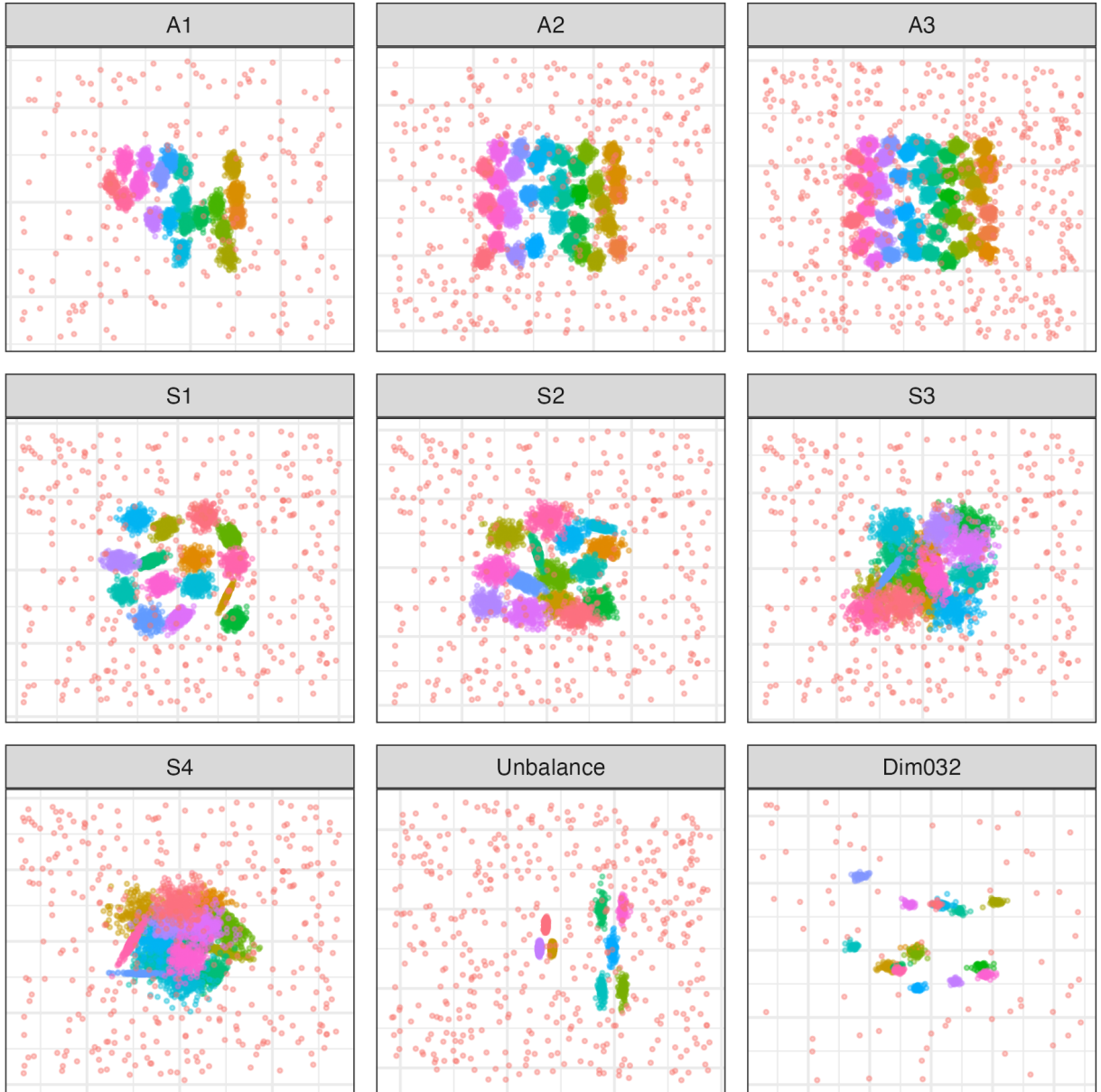


Figure 3: The nine benchmark datasets used herein, where red points represent added uniform noise and other colours correspond to the true classes.

2018) with default  $k$ -means initialization. The `CNmixt` function chooses the best model for variance and contamination using the BIC. We run NCM using the `Mclust` function in the `mclust` package (Scrucca et al., 2016), initializing the noise component as a random sample of points with probability  $1/4$ . We let the package choose the best model using the Bayesian information criterion (Schwarz, 1978). We run mean-shift outlier detection in Python using Yang (n.d.)’s code. We specify the number of clusters and perform three iterations. Due

to its superior performance in Fränti and Yang (2018), non-outlying points are clustered using random swap clustering in Python (Yang et al., 2021; Fränti, 2018) and run for the recommended 5000 iterations. We implement the DBSCAN algorithm with the `dbscan` package, setting the minimum number of points per cluster to be 20. For the thresholding approach, we calculate the squared Mahalanobis distance from the centre of the dataset and trim those that are more than three standard deviations away from the mean. This is performed twice, and the remaining points are clustered with the `mixture` package.

The performance of each method can be assessed using three approaches for evaluating classification accuracy — adjusted Rand index (ARI; Hubert and Arabie, 1985), normalized mutual information (NMI; Kvalseth, 1987), and centroid index (CI; Fränti et al., 2014) — and two approaches of outlier detection performance — true positive rate (TPR) and false positive rate (FPR). The ARI is a measure of agreement between two partitions, e.g., between clusters and true classes. The ARI equals 1 with perfect agreement and has expected value 0 when randomly partitioned. Negative values indicate partitions with less agreement than would be expected by random chance. NMI is a measure of the amount of information shared between the true classes and the clustering solution. It is a scale from 0 to 1, with 0 corresponding to no mutual information and 1 corresponding to perfect agreement. CI is a measure of dissimilarity among cluster centroids, where  $CI = 0$  reflects one-to-one correspondence between the estimated cluster centres and the ground truth. We calculate ARI and NMI for cluster agreement taking into account whether points are classified into the correct group, considering outliers as one of those groups. TPR reflects the proportion of true outliers classified as such and FPR reflects the proportion of non-outliers classified as outliers. The results are shown in Table 2, with the best algorithm according to each approach bolded.

For datasets with many clusters, i.e., A2 and A3, OCLUST does better than its competitors. OCLUST and mean-shift have  $CI = 0$  for all but one dataset. Mean-shift performs better than the Gaussian model-based approaches as the clusters become highly overlapped in S4. The model-based approaches cannot recover symmetric distributions, such as the Gaussian distribution, for each component when the clusters severely overlap. The OCLUST and mean-shift algorithms attain similar results on the A1, S1, S2, and S3 datasets. Mean-shift performs well, as expected, for those datasets because the clusters are spherical and well-separated. With the exception of DBSCAN, most of the algorithms have a nearly zero FPR. DBSCAN has a perfect TPR for four of the datasets, but this is also accompanied by a very large FPR, indicating that DBSCAN is considering most points to be outliers for those datasets. After discarding these results from DBSCAN, OCLUST has the largest TPR for most of the datasets.

OCLUST, mean-shift, and NCM perform very well on the 32-dimensional dataset, likely due to the uniform generation of outliers. This is because, as the dimensionality increases, it is more likely for a generated outlier to be far from the clusters in any one direction. OCLUST, CNMix, NCM, and DBSCAN perform well on the Unbalance dataset. Mean-shift filters most of the Unbalance points as noise, resulting in poor classification. DBSCAN performs poorly on most datasets, often over-specifying the number of outliers and combining clusters together. The thresholding approach performs consistently for outlier identification

Table 2: Results of the six outlier identification algorithms on the benchmark datasets. ARI and NMI consider cluster classification with ‘outlier’ being considered a class.

A1 Dataset						A2 Dataset					
Algorithm	ARI	NMI	CI	TPR	FPR	Algorithm	ARI	NMI	CI	TPR	FPR
OCLUST	0.96	0.97	<b>0</b>	<b>0.87</b>	<b>0.00</b>	OCLUST	<b>0.95</b>	<b>0.97</b>	<b>0</b>	<b>0.82</b>	<b>0.00</b>
Mean-Shift	<b>0.97</b>	<b>0.98</b>	<b>0</b>	0.82	<b>0.00</b>	Mean-Shift	0.94	<b>0.97</b>	<b>0</b>	0.73	<b>0.00</b>
2T	0.84	0.92	1	0.69	<b>0.00</b>	2T	0.81	0.93	4	0.68	<b>0.00</b>
CNMix	0.74	0.86	5	0.00	<b>0.00</b>	CNMix	0.72	0.89	7	0.00	<b>0.00</b>
NCM	0.79	0.89	3	0.80	<b>0.00</b>	NCM	0.55	0.75	17	0.60	<b>0.00</b>
DBSCAN	0.01	0.06	19	0.85	<b>0.00</b>	DBSCAN	0.00	0.04	34	0.73	<b>0.00</b>

A3 Dataset						S1 Dataset					
Algorithm	ARI	NMI	CI	TPR	FPR	Algorithm	ARI	NMI	CI	TPR	FPR
OCLUST	<b>0.94</b>	<b>0.97</b>	<b>0</b>	<b>0.83</b>	<b>0.00</b>	OCLUST	<b>0.96</b>	<b>0.96</b>	<b>0</b>	0.89	0.01
Mean-Shift	0.93	<b>0.97</b>	<b>0</b>	0.72	<b>0.00</b>	Mean-Shift	0.95	<b>0.96</b>	<b>0</b>	0.87	0.01
2T	0.84	0.95	4	0.67	<b>0.00</b>	2T	0.95	<b>0.96</b>	<b>0</b>	0.72	<b>0.00</b>
CNMix	0.72	0.90	11	0.00	<b>0.00</b>	CNMix	0.80	0.87	2	0.00	<b>0.00</b>
NCM	0.53	0.76	26	0.56	<b>0.00</b>	NCM	0.90	0.93	1	0.85	<b>0.00</b>
DBSCAN	-0.00	0.04	49	0.68	<b>0.00</b>	DBSCAN	0.01	0.18	<b>0</b>	<b>1.00</b>	0.81

S2 Dataset						S3 Dataset					
Algorithm	ARI	NMI	CI	TPR	FPR	Algorithm	ARI	NMI	CI	TPR	FPR
OCLUST	0.91	0.92	<b>0</b>	0.81	<b>0.00</b>	OCLUST	<b>0.72</b>	<b>0.79</b>	<b>0</b>	0.85	0.01
Mean-Shift	<b>0.92</b>	<b>0.93</b>	<b>0</b>	0.84	<b>0.00</b>	Mean-Shift	0.71	0.78	<b>0</b>	0.83	0.01
2T	0.70	0.83	1	0.73	<b>0.00</b>	2T	0.42	0.67	1	0.73	<b>0.00</b>
CNMix	0.72	0.82	3	0.07	0.02	CNMix	0.54	0.69	4	0.00	<b>0.00</b>
NCM	0.86	0.90	1	0.82	<b>0.00</b>	NCM	0.55	0.72	3	0.80	<b>0.00</b>
DBSCAN	0.01	0.13	2	<b>1.00</b>	0.87	DBSCAN	0.01	0.07	9	<b>1.00</b>	0.93

S4 Dataset						Unbalance Dataset					
Algorithm	ARI	NMI	CI	TPR	FPR	Algorithm	ARI	NMI	CI	TPR	FPR
OCLUST	0.42	0.65	1	0.91	0.02	OCLUST	<b>1.00</b>	<b>0.99</b>	<b>0</b>	0.96	<b>0.00</b>
Mean-Shift	<b>0.63</b>	<b>0.72</b>	<b>0</b>	0.86	0.01	Mean-Shift	0.43	0.58	5	<b>1.00</b>	0.10
2T	0.16	0.50	1	0.79	<b>0.00</b>	2T	0.88	0.85	3	0.80	0.01
CNMix	0.40	0.59	4	0.00	<b>0.00</b>	CNMix	0.99	0.94	3	0.00	<b>0.00</b>
NCM	0.56	0.69	2	0.83	<b>0.00</b>	NCM	0.99	0.96	2	0.91	<b>0.00</b>
DBSCAN	0.01	0.11	8	<b>1.00</b>	0.89	DBSCAN	0.98	0.91	<b>0</b>	0.99	0.05

Dim032 Dataset					
Algorithm	ARI	NMI	CI	TPR	FPR
OCLUST	0.99	0.99	<b>0</b>	<b>1.00</b>	<b>0.00</b>
Mean-Shift	<b>1.00</b>	<b>1.00</b>	<b>0</b>	<b>1.00</b>	<b>0.00</b>
2T	0.71	0.87	4	<b>1.00</b>	<b>0.00</b>
CNMix	0.07	0.38	1	0.99	0.60
NCM	0.98	0.99	<b>0</b>	<b>1.00</b>	0.01
DBSCAN	0.00	0.00	15	0.00	<b>0.00</b>

but fails when clusters become more overlapped, likely due to remaining outliers reducing clustering performance.

In Figure 4, the KL graph for the A3 dataset is plotted. It displays a typical shape, decreasing to a minimum at 446 outliers, after which KL increases. The minimum at 446 is notably different from 525, the number of outliers generated. However, this is to be expected due to the uniform generation of outliers because many of them overlap with the clusters as seen in Figure 3. All the algorithms experience the same issue in this respect.

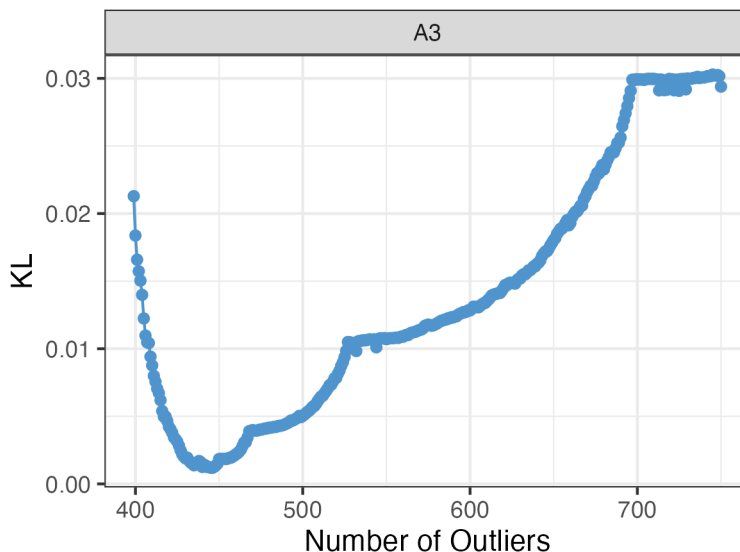


Figure 4: KL plot for the A3 dataset, where the minimum is at 446 outliers.

In the initial gross outlier removal for the A3 dataset, 399 outliers are removed. We reach a minimum KL divergence after 48 iterations, but continuing until  $F = 750$  requires a further 304 iterations. At the minimum KL divergence, we achieve an approximate p-value of 0.099 on Kuiper’s test when  $m = 100$ . If our significance level was 0.05, we would be able to stop here and substantially save computation time.

### 4.3 Crabs Study

Next we evaluate the sensitivity of OCLUST using the crabs dataset (Campbell and Mahon, 1974), which is available in the MASS package (Venables and Ripley, 2002). This study closely mimics the study carried out by Peel and McLachlan (2000) and again by Punzo and McNicholas (2016) to demonstrate their respective approaches to dealing with outliers in model-based clustering. The dataset contains observations for 100 blue crabs, 50 of which are male, and 50 of which are female. The aim for each classification is to recover the sex of the crab. For this study, we will focus on measurements of rear width (RW) and carapace length (CL). We substitute the CL value of the 25th point to one of eight values in  $[-15, 20]$ . The leftmost plot in Figure 5 plots the crabs dataset by sex, with the permuted value in red taking value  $CL = -5$ . We use the OCLUST, mean-shift, CNMix, NCM, and DBSCAN

algorithms, along with the thresholding approach. For OCLUST, CNMix and NCM, we run each method, restricting the model to one where the clusters have equal shapes and volumes but varying orientations. We let the `CNmixt` function determine whether or not the CNMix model is contaminated. Solutions for OCLUST, CNMix, NCM, and the thresholding approach (2T) for the dataset with  $CL = -5$  are plotted in Figure 5. Table 3 summarizes the results for each method, listing the number of misclassified points (M) and the predicted number of outliers ( $n_O$ ).

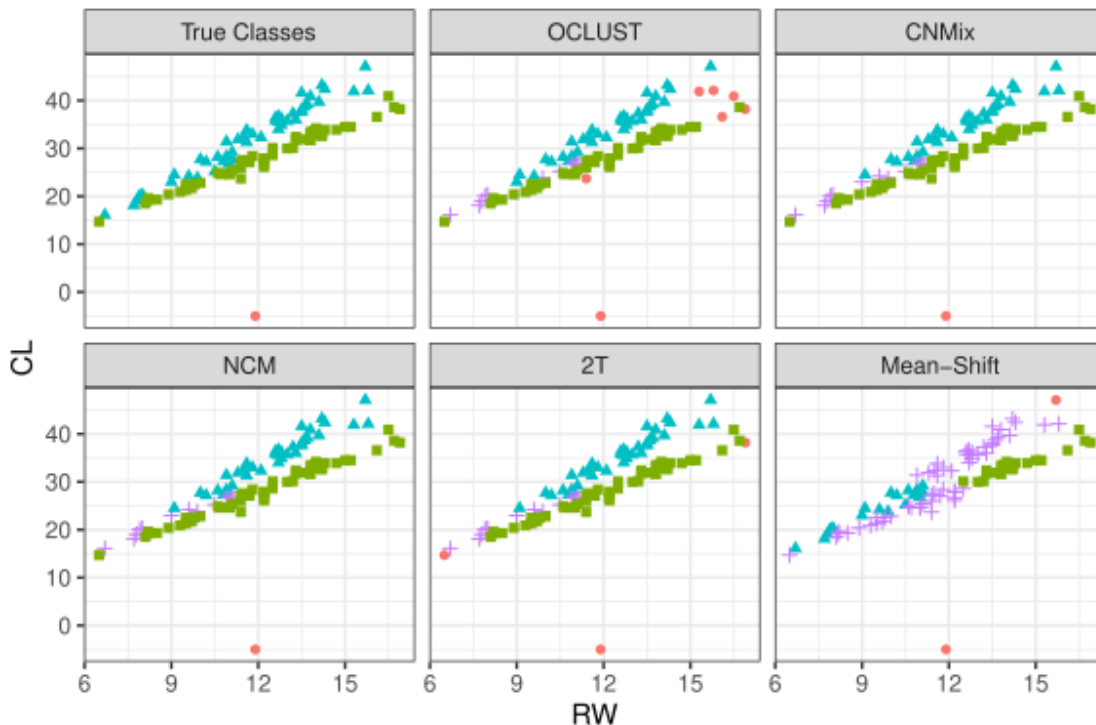


Figure 5: Predicted classifications for OCLUST, CNMix, NCM, mean-shift, and the thresholding approach (2T) when  $CL = -5$ . Green squares, blue triangles, purple crosses, and red circles indicate female, male, misclassified, and outlying points, respectively.

Each method, with the exception of DBSCAN, always identifies the permuted value correctly as an outlier. DBSCAN clusters all the data, including the outlier, into one cluster. NCM classifies more points as outliers as the permuted  $CL$  value becomes less extreme. In contrast, OCLUST does the reverse because when the outlier is farther away, it is removed in the gross outlier stage. A gross outlier does not affect the initial clustering, allowing the OCLUST algorithm to remove more points that deviate from multivariate normality.

OCLUST identifies more points as outliers than its competitors and has fewer misclassifications in most instances. It is important to note that the outliers found by OCLUST are not simply the misclassifications — i.e., outliers classified as non-outliers and *vice versa* — of NCM. Instead, as seen in Figure 5, OCLUST identifies three points between the clusters as outliers. This removes the points with high leverage, allowing the clusters to rotate and

Table 3: Results for running each method on the crabs dataset, where ‘M’ and ‘ $n_O$ ’ designate the number of misclassified points and number of predicted outliers, respectively.

CL	OCLUST		Mean-Shift		2T		CNMix		NCM		DBSCAN	
	M	$n_O$	M	$n_O$	M	$n_O$	M	$n_O$	M	$n_O$	M	$n_O$
-15	11	8	41	3	12	4	13	1	13	1	50	0
-10	11	6	41	3	13	3	13	1	13	1	50	0
-5	11	7	41	3	13	3	13	1	13	1	50	0
0	11	4	41	3	13	2	13	1	13	1	50	0
5	12	5	41	3	13	3	13	1	13	2	50	0
10	11	4	41	3	13	3	13	1	11	3	50	0
15	11	5	41	3	13	3	13	1	10	4	50	0
20	11	5	42	2	14	4	13	1	9	5	50	0

improve the classification among low values of RW. From one point of view, one may consider that OCLUST removes a few more outliers than necessary; however, their removal improves the parameter estimates. The thresholding approach cannot identify mild outliers because it detects outliers before clustering. Mean shift performs poorly for this dataset due to the shape of the clusters.

#### 4.4 Wine Data

Finally, we evaluate the results of OCLUST on the wine dataset, available in the `gclus` package (Hurley, 2019). This dataset describes 13 attributes of 178 Italian wines (e.g., alcohol, hue, malic acid). Each wine originates from one of three cultivars: Barolo, Barbera, or Grignolino. For this analysis, we add 12 points of noise, uniformly distributed in each dimension as described in Section 4.2. We perform unsupervised classification on this dataset with the aim of removing the noise and recovering the cultivar for each wine. We run OCLUST as well as the five comparator methods from Section 4.3. The results for the comparators, except DBSCAN, are provided in Table 4. DBSCAN performs poorly by classifying all points into one cluster and only identifying seven points of added noise.

NCM achieves good results, with only six misclassifications, five of which are from the Grignolino cultivar. It identifies all 12 points of added noise as outliers. CNMix identifies all 12 outliers and has fewer misclassifications than NCM, all four of which are from the Grignolino cultivar. The thresholding approach performs very well, likely due to the uniform simulation of noise in 13 dimensions creating gross outliers. Mean-shift performs poorly.

The solution for OCLUST, with the minimum KL divergence, is shown in Table 4. We have perfect classification among the good points, but 76 points are treated as outliers, which represents 40% of the dataset. Our KL divergence graph in Figure 6a has a local minimum at around 35 outliers, which could be viewed as good alternative solution with fewer outliers. Re-running the OCLUST algorithm with our p-value stopping criterion results in it stopping at 35 outliers with p-value 0.059. The classification results with 35 outliers are shown in Table 4. This allows for the preservation of more original data with minimal

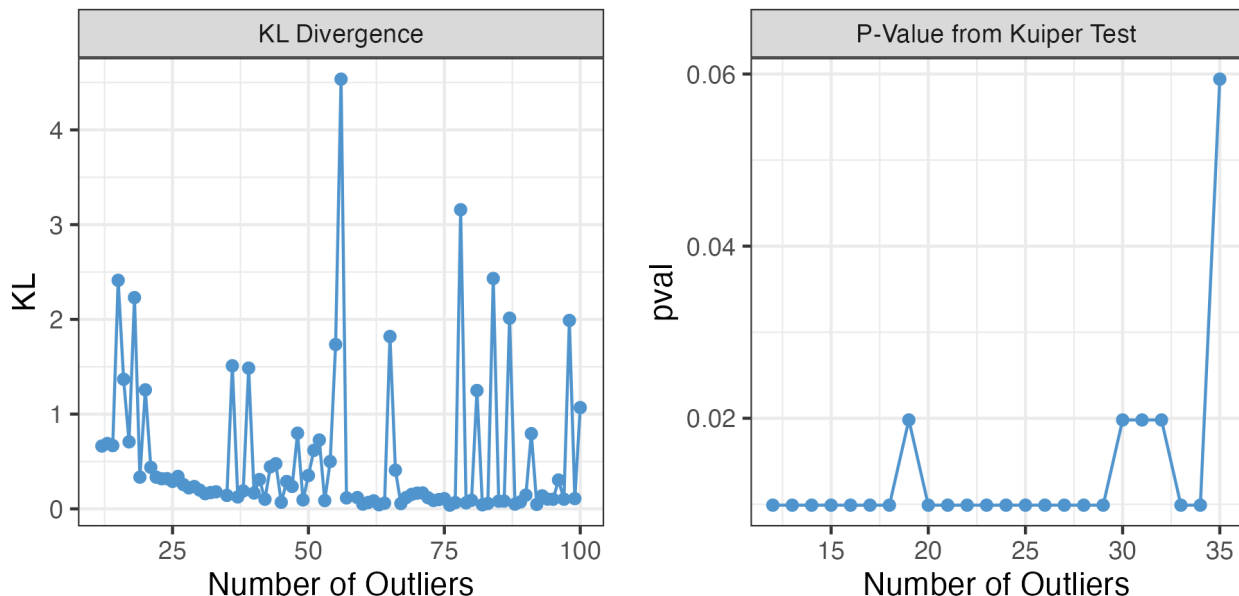
Table 4: Classification results for CNMix, NCM, 2T, mean-shift and OCLUS T on the wine dataset. Classification results on the wine dataset for OCLUS T at global minimum KL and when stopped when the p-value exceeds 0.05.

Cultivar	CNMix				NCM				2T			
	1	2	3	bad	1	2	3	bad	1	2	3	bad
Barbera	47			1	47			1	48			
Barolo		59				58	1			59		
Grignolino	4		58	9	3	2	65	1	5	1	65	
Noise				12				12				12
Cultivar	Mean-Shift				OCLUS T Min. KL				OCLUS T p-val>0.05			
	1	2	3	bad	1	2	3	bad	1	2	bad	
Barbera	29		19		33			15	44		4	
Barolo	13	44		2		43		16		58	1	
Grignolino	19	1	50	1			38	33	2		51	18
Noise	1			11				12				12

decrease in classification accuracy. This alternative solution has fewer misclassifications than its comparators.

The associated KL divergence plot (Figure 6a) displays a pattern unlike Figure 4 because the data are real and not perfectly multivariate normal. We tested each cluster for multivariate normality when all 76 outliers are removed and at the intermediate solution with 35 outliers. We tested the null hypothesis of multivariate normality using the energy test in the `energy` package (Székely and Rizzo, 2013; Rizzo and Székely, 2022). When 35 outliers are removed, the Barolo, Barbera, and Grignolino clusters have p-values of 0.09, 0.27, and 0.09, respectively. At the minimum KL solution, i.e., with 76 points removed, the Barolo, Barbera, and Grignolino clusters have p-values of 0.77, 0.35, and 0.59, respectively. Evidently, OCLUS T continues to remove points until the clusters are unmistakably multivariate normal.

Two-dimensional projections of both OCLUS T solutions are shown in Figure 7. In the left-hand figure, where only 35 points are removed, we see some of the identified outliers are far from the clusters but others are mild outliers. In the right-hand plot, we see the solution when more points are removed. Although they may have been correctly classified, they deviate from the symmetric elliptic shape of the multivariate Gaussian distribution. The competing Gaussian model-based classification algorithms, i.e., CNMix and NCM, are able to correctly cluster these points but they seem not to fit well within the model. Identifying these additional outliers may be useful in novelty detection. These wines present inconsistent features which may be relevant to quality control. The spurious points do not fit into the model and indicate wines with chemical and physical properties that differ from the rest.



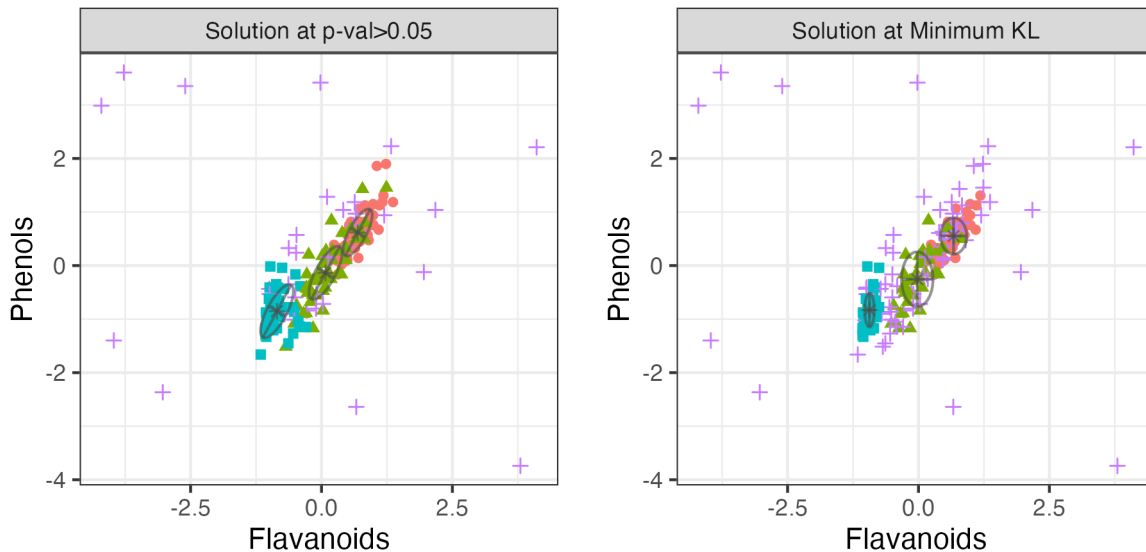
(a) KL plot for the wine dataset. The algorithm is run to an upper bound of 100 outliers. (b) P-value plot for the wine dataset. The algorithm is stopped at 35 outliers because the p-value exceeds 0.05

Figure 6: KL and p-value plots, respectively, for the wine dataset.

## 5 Discussion

It was shown that, for data from a finite Gaussian mixture model, the log-likelihoods of the subset models are approximately distributed according to a mixture of beta distributions. This result was used to identify outliers, without needing specification of the proportion of outliers, by removing outlying points until the subset log-likelihoods followed this derived distribution. The result is the OCLUS algorithm, which trims outliers from a dataset while clustering using Gaussian mixture models. In simulations, OCLUS performs similarly or better than mean-shift outlier detection for most benchmark datasets except where there is extreme cluster overlap, i.e., S3 and S4. OCLUS performs similarly to NCM when the clusters are elliptical in the real datasets. For the crabs data, OCLUS trims mild outliers with high leverage, which improves the classification for small values of CL. For the wine dataset, OCLUS obtains good classification with fewer iterations. However, if the algorithm is allowed to continue, it removes points which deviate from the assumption of multivariate normality, arguably removing too many points in the process.

Although this work used the distribution of the log-likelihoods of the subset models to test for the presence of outliers, the derived distribution may be used to verify other underlying model assumptions, such as whether the clusters are Gaussian. Note that the OCLUS algorithm could be used with other clustering methods and should be effective so long as it is reasonable to assume that the underlying distribution of clusters is Gaussian. Of course, one could extend this work by deriving the distribution of subset log-likelihoods for mixture



(a) OCLUS T classification with 35 identified outliers. (b) OCLUS T classification with 76 identified outliers.

Figure 7: Predicted classifications by the OCLUS T algorithm for the wine dataset with 12 uniform outliers simulated. Scaled data are plotted in two dimensions, showing measurements for flavanoids and phenols. Purple crosses indicate the predicted outliers.

models with non-Gaussian components. This would allow direct consideration of asymmetric clusters with outliers. Finally, this model is limited by dimensionality because, without sufficient observations, the underlying mixture model becomes over parametrized. One could extend this approach to high-dimensional data by using an analogue of the mixture of factor analyzers model or its extensions (see, e.g., [Ghahramani and Hinton, 1997](#); [McNicholas and Murphy, 2008, 2010](#)). Based on the comparisons conducted herein, one might expect the resulting method to perform favourably, or at least comparably, when compared to the approaches used by [Wei and Yang \(2012\)](#) and [Punzo et al. \(2020\)](#).

## Acknowledgments

This work was supported by an NSERC Undergraduate Research Award, an NSERC Canada Graduate Scholarship, the Canada Research Chairs program, an E.W.R. Steacie Memorial Fellowship, and a Dorothy Killam Fellowship.

## References

- Andrews, J. L. and McNicholas, P. D. (2011a). “Extending mixtures of multivariate t-factor analyzers.” *Statistics and Computing*, 21(3): 361–373 (2011).
- Bagnato, L., Punzo, A., and Zoia, M. G. “The multivariate leptokurtic-normal distribution

- and its application in model-based clustering.” *Canadian Journal of Statistics*, 45(1):95–119 (2017).
- Banfield, J. D. and Raftery, A. E. “Model-based Gaussian and non-Gaussian clustering.” *Biometrics*, 49(3):803–821 (1993).
- Boukerche, A., Zheng, L., and Alfandi, O. “Outlier detection: Methods, models, and classification.” *ACM Computing Surveys (CSUR)*, 53(3):1–37 (2020).
- Buzzi-Ferraris, G. and Manenti, F. “Outlier detection in large data sets.” *Computers & Chemical Engineering*, 35(2):388–390 (2011).
- Campbell, N. A. and Mahon, R. J. “A Multivariate Study of Variation in Two Species of Rock Crab of Genus *Leptograpsus*.” *Australian Journal of Zoology*, 22:417–425 (1974).
- Clark, K. M. and McNicholas, P. D. *oclust: Gaussian Model-Based Clustering with Outliers* (2022). R package version 0.2.0.  
URL <https://CRAN.R-project.org/package=oclust>
- Cuesta-Albertos, J. A., Gordaliza, A., and Matrán, C. “Trimmed  $k$ -means: an attempt to robustify quantizers.” *The Annals of Statistics*, 25(2):553–576 (1997).
- Dang, U. J., Browne, R. P., and McNicholas, P. D. “Mixtures of Multivariate Power Exponential Distributions.” *Biometrics*, 71(4):1081–1089 (2015).
- Dempster, A. P., Laird, N. M., and Rubin, D. B. “Maximum likelihood from incomplete data via the EM algorithm.” *Journal of the Royal Statistical Society: Series B*, 39(1):1–38 (1977).
- Domingues, R., Filippone, M., Michiardi, P., and Zouaoui, J. “A comparative evaluation of outlier detection algorithms: Experiments and analyses.” *Pattern Recognition*, 74:406–421 (2018).
- Ester, M., Kriegel, H.-P., Sander, J., and Xu, X. “A density-based algorithm for discovering clusters in large spatial databases with noise.” In *Proceedings of the Second International Conference on Knowledge Discovery and Data Mining (KDD-96)*, 226–231. AAAI Press (1996).
- Evans, K., Love, T., and Thurston, S. W. “Outlier identification in model-based cluster analysis.” *Journal of Classification*, 32(1):63 (2015).
- Fränti, P. “Efficiency of random swap clustering.” *Journal of Big Data*, 5(1):13 (2018).
- Fränti, P., Rezaei, M., and Zhao, Q. “Centroid index: Cluster level similarity measure.” *Pattern Recognition*, 47(9):3034–3045 (2014).
- Fränti, P. and Sieranoja, S. “K-means properties on six clustering benchmark datasets.” *Applied Intelligence*, 48(12):4743–4759 (2018).

- Fränti, P. and Yang, J. “Medoid-Shift for Noise Removal to Improve Clustering.” In *International Conference on Artificial Intelligence and Soft Computing*, 604–614. Springer (2018).
- García-Escudero, L. A., Gordaliza, A., Matrán, C., and Mayo-Iscar, A. “A General Trimming Approach to Robust Cluster Analysis.” *The Annals of Statistics*, 36(3):1324–1345 (2008).
- García-Escudero, L. A., Gordaliza, A., Matrán, C., and Mayo-Iscar, A. “Exploring the Number of Groups in Robust Model-Based Clustering.” *Statistics and Computing*, 21(4):585–599 (2011).
- Ghahramani, Z. and Hinton, G. E. “The EM algorithm for factor analyzers.” Technical Report CRG-TR-96-1, University of Toronto, Toronto, Canada (1997).
- Gnanadesikan, R. and Kettenring, J. R. “Robust Estimates, Residuals, and Outlier Detection with Multiresponse Data.” *Biometrics*, 28(1):81–124 (1972).
- Grubbs, F. E. “Procedures for detecting outlying observations in samples.” *Technometrics*, 11(1):1–21 (1969).
- Hahsler, M., Piekenbrock, M., and Doran, D. “dbscan: Fast Density-Based Clustering with R.” *Journal of Statistical Software*, 91(1):1–30 (2019).
- Hampel, F. R. “The influence curve and its role in robust estimation.” *Journal of the American Statistical Association*, 69(346):383–393 (1974).
- Hautamäki, V., Cherednichenko, S., Kärkkäinen, I., Kinnunen, T., and Fränti, P. “Improving k-means by outlier removal.” In *Scandinavian Conference on Image Analysis*, 978–987. Springer (2005).
- Hubert, L. and Arabie, P. “Comparing Partitions.” *Journal of Classification*, 2(1):193–218 (1985).
- Hurley, C. *gclus: Clustering Graphics* (2019). R package version 1.3.2.  
URL <https://CRAN.R-project.org/package=gclus>
- Knorr, E. M. and Ng, R. T. “Algorithms for mining distance-based outliers in large datasets.” In *VLDB*, volume 98, 392–403. Citeseer (1998).
- Kuiper, N. H. “Tests concerning random points on a circle.” *Indagationes Mathematicae (Proceedings)*, 63: 38–47 (1960).
- Kvalseth, T. O. “Entropy and correlation: Some comments.” *IEEE Transactions on Systems, Man, and Cybernetics*, 17(3):517–519 (1987).
- McNicholas, P. D. *Mixture Model-Based Classification*. Boca Raton: Chapman and Hall/CRC Press (2016a).

- McNicholas, P. D. “Model-based clustering.” *Journal of Classification*, 33(3):331–373 (2016b).
- McNicholas, P. D. and Murphy, T. B. “Parsimonious Gaussian mixture models.” *Statistics and Computing*, 18(3):285–296 (2008).
- McNicholas, P. D. and Murphy, T. B. “Model-based clustering of microarray expression data via latent Gaussian mixture models.” *Bioinformatics*, 26(21):2705–2712 (2010).
- North, B. V., Curtis, D., and Sham, P. C. “A note on the calculation of empirical P values from Monte Carlo procedures.” *The American Journal of Human Genetics*, 71(2):439–441 (2002).
- Peel, D. and McLachlan, G. J. “Robust mixture modelling using the t distribution.” *Statistics and Computing*, 10(4):339–348 (2000).
- Pimentel, M. A. F., Clifton, D. A., Clifton, L., and Tarassenko, L. “A review of novelty detection.” *Signal Processing*, 99:215–249 (2014).
- Pocuca, N., Browne, R. P., and McNicholas, P. D. *mixture: Mixture Models for Clustering and Classification* (2024). R package version 2.1.1.  
URL <https://CRAN.R-project.org/package=mixture>
- Punzo, A., Blostein, M., and McNicholas, P. D. “High-dimensional unsupervised classification via parsimonious contaminated mixtures.” *Pattern Recognition*, 98:107031 (2020).
- Punzo, A., Mazza, A., and McNicholas, P. D. “ContaminatedMixt: An R Package for Fitting Parsimonious Mixtures of Multivariate Contaminated Normal Distributions.” *Journal of Statistical Software*, 85(10):1–25 (2018).
- Punzo, A. and McNicholas, P. D. “Parsimonious mixtures of multivariate contaminated normal distributions.” *Biometrical Journal*, 58(6):1506–1537 (2016).
- Qiu, W. and Joe, H. “Separation index and partial membership for clustering.” *Computational Statistics & Data Analysis*, 50(3):585–603 (2006).
- Qiu, W. and Joe, H. *clusterGeneration: Random Cluster Generation (with Specified Degree of Separation)* (2015). R package version 1.3.4.  
URL <https://CRAN.R-project.org/package=clusterGeneration>
- R Core Team. *R: A Language and Environment for Statistical Computing*. R Foundation for Statistical Computing, Vienna, Austria (2023).  
URL <https://www.R-project.org/>
- Ramaswamy, S., Rastogi, R., and Shim, K. “Efficient algorithms for mining outliers from large data sets.” In *Proceedings of the 2000 ACM SIGMOD international conference on Management of data*, 427–438 (2000).

- Ritter, G. *Robust Cluster Analysis and Variable Selection*, London: Chapman and Hall/CRC Press (2014).
- Rizzo, M. and Székely, G. *energy: E-Statistics: Multivariate Inference via the Energy of Data* (2022). R package version 1.7-11.  
URL <https://CRAN.R-project.org/package=energy>
- Schwarz, G. “Estimating the dimension of a model.” *The Annals of Statistics*, 6(2): 461–464 (1978).
- Scrucca, L., Fop, M., Murphy, T. B., and Raftery, A. E. “mclust 5: Clustering, classification and density estimation using Gaussian finite mixture models.” *The R Journal*, 8(1):205–233 (2016).
- Sun, J., Kabán, A., and Garibaldi, J. M. “Robust mixture clustering using Pearson type VII distribution.” *Pattern Recognition Letters*, 31:2447–2454 (2010).
- Székely, G. J. and Rizzo, M. L. “Energy statistics: A class of statistics based on distances.” *Journal of Statistical Planning and Inference*, 143(8):1249–1272 (2013).
- Tomarchio, S. D., Bagnato, L., and Punzo, A. “Model-based clustering via new parsimonious mixtures of heavy-tailed distributions.” *ASTA Advances in Statistical Analysis*, 106: 315–347 (2022).
- Venables, W. N. and Ripley, B. D. *Modern Applied Statistics with S*, 4th ed. New York: Springer (2016).
- Ververidis, D. and Kotropoulos, C. “Gaussian mixture modeling by exploiting the Mahalanobis distance.” *IEEE Transactions on Signal Processing*, 56(7):2797–2811 (2008).
- Wei, X. and Yang, Z. “The infinite Student’s t-factor mixture analyzer for robust clustering and classification.” *Pattern Recognition*, 45:4346–4357 (2012).
- Yang, J. “MeanShift-OD.” <http://cs.uef.fi/sipu/soft/MeanShift-OD.py> (n.d.).
- Yang, J., Rahardja, S., and Fränti, P. “Outlier detection: how to threshold outlier scores?” In *Proceedings of the International Conference on Artificial Intelligence, Information Processing and Cloud Computing*, 37, (2019).
- Yang, J., Rahardja, S., and Fränti, P. “Mean-shift outlier detection and filtering.” *Pattern Recognition*, 115:107874 (2021).

## A Relaxing Assumptions

Lemma 1 assumes that the clusters are well separated and non-overlapping to simplify the model density to the component density. This appendix, however, serves to show that this assumption may be relaxed in practice. Following Qiu and Joe (2006), we can quantify the separation between clusters using the separation index  $J^*$ . In the univariate case,

$$J^* = \frac{L_2(\alpha/2) - U_1(\alpha/2)}{U_2(\alpha/2) - L_1(\alpha/2)},$$

where  $L_i(\alpha/2)$  is the sample lower  $\alpha/2$  quantile and  $U_i(\alpha/2)$  is the sample upper  $\alpha/2$  quantile of cluster  $i$ , and cluster 1 has lower mean than cluster 2. In the multivariate case, the separation index is calculated along the projected direction of maximum separation. Clusters with  $J^* > 0$  are separated, clusters with  $J^* < 0$  overlap, and clusters with  $J^* = 0$  are touching.

To measure the effect of separation index  $J^*$  on the complete-data log-likelihood  $l_{\mathcal{X}}$ , 100 random datasets with  $n = 1800$  for each combination of settings used were generated using the `clusterGeneration` (Qiu and Joe, 2015) package in R. The settings used were: three clusters with equal cluster proportions, dimensions  $p \in \{2, 4, 6\}$ , and separation indices in  $[-0.9, 0.9]$ . Covariance matrices were generated using random eigenvalues  $\lambda \in (0, 10]$ . The parameters were estimated using the EM algorithm. The log-likelihood and the complete-data log-likelihood were calculated using the parameter estimates. The average of the quantity  $(l_{\mathcal{X}} - \ell_{\mathcal{X}})/\ell_{\mathcal{X}}$  is computed for each combination of settings — recall that there are 100 datasets for each setting. The result is the average proportional change in log-likelihood over the 100 datasets between the log-likelihood  $\ell_{\mathcal{X}}$  and the complete-data log-likelihood  $l_{\mathcal{X}}$  (Figure 8).

As one would expect, the approximation of  $\ell_{\mathcal{X}}$  by  $l_{\mathcal{X}}$  improves as the separation index increases (see Lemma 1). However, the difference is negligible for touching and separated clusters ( $J^* \geq 0$ ).

## B Mathematical Results

### B.1 Proof of Lemma 1

*Proof.* Suppose  $\Sigma$  is positive definite. Then,  $\Sigma^{-1}$  is also positive definite and there exists a matrix  $\mathbf{Q}$  such that  $\mathbf{Q}'\mathbf{Q} = \mathbf{I}$  and  $\Sigma^{-1} = \mathbf{Q}'\mathbf{\Lambda}\mathbf{Q}$ , where  $\mathbf{\Lambda}$  is diagonal with  $\Lambda_{ii} = \lambda_i > 0, i \in [1, p]$ . Let  $\mathbf{x} - \boldsymbol{\mu} = \mathbf{Q}'\mathbf{w}$ , where  $\mathbf{w} \neq \mathbf{0}$ . Now,

$$\begin{aligned} (\mathbf{x} - \boldsymbol{\mu})'\Sigma^{-1}(\mathbf{x} - \boldsymbol{\mu}) &= \mathbf{w}'\mathbf{Q}\Sigma^{-1}\mathbf{Q}'\mathbf{w} = \mathbf{w}'\mathbf{\Lambda}\mathbf{w} = \sum_{i=1}^p \lambda_i w_i^2 \\ &\geq \inf_i(\lambda_i) \sum_{i=1}^p w_i^2 = \inf_i(\lambda_i) \|\mathbf{w}\|^2 = \inf_i(\lambda_i) \|\mathbf{x} - \boldsymbol{\mu}\|^2 \end{aligned}$$

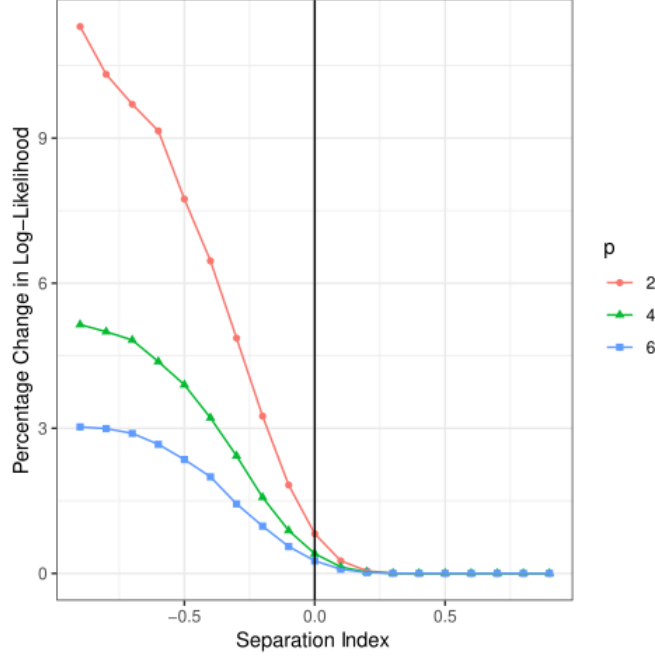


Figure 8: The effect of cluster separation on the complete-data log-likelihood of the model, where the vertical line represents the threshold between separated and overlapping clusters.

because  $\|\mathbf{x} - \boldsymbol{\mu}\|^2 = \|\mathbf{Q}'\mathbf{w}\|^2 = \mathbf{w}'\mathbf{Q}\mathbf{Q}'\mathbf{w} = \|\mathbf{w}\|^2$ . Thus, as  $\|\mathbf{x} - \boldsymbol{\mu}\| \rightarrow \infty$ ,

$$(\mathbf{x} - \boldsymbol{\mu})' \boldsymbol{\Sigma}^{-1} (\mathbf{x} - \boldsymbol{\mu}) \rightarrow \infty$$

and

$$\phi(\mathbf{x} \mid \boldsymbol{\mu}, \boldsymbol{\Sigma}) = \frac{1}{\sqrt{(2\pi)^p |\boldsymbol{\Sigma}|}} \exp \left\{ -\frac{1}{2} (\mathbf{x} - \boldsymbol{\mu})' \boldsymbol{\Sigma}^{-1} (\mathbf{x} - \boldsymbol{\mu}) \right\} \rightarrow 0.$$

Suppose  $z_{ih} = 1$ . Then, as the clusters separate,  $\|\mathbf{x}_i - \boldsymbol{\mu}_g\| \rightarrow \infty$  and  $\phi(\mathbf{x}_i \mid \boldsymbol{\mu}_g, \boldsymbol{\Sigma}_g) \rightarrow 0$  for  $g \neq h$ . Thus, for  $\mathbf{x}_i$ ,

$$\sum_{g=1}^G \pi_g \phi(\mathbf{x}_i \mid \boldsymbol{\mu}_g, \boldsymbol{\Sigma}_g) = \sum_{g \neq h} \pi_g \phi(\mathbf{x}_i \mid \boldsymbol{\mu}_g, \boldsymbol{\Sigma}_g) + \pi_h \phi(\mathbf{x}_i \mid \boldsymbol{\mu}_h, \boldsymbol{\Sigma}_h) \rightarrow \pi_h \phi(\mathbf{x}_i \mid \boldsymbol{\mu}_h, \boldsymbol{\Sigma}_h)$$

as  $\|\mathbf{x}_i - \boldsymbol{\mu}_g\| \rightarrow \infty, g \neq h$ . Therefore,

$$\ell_{\mathcal{X}} = \sum_{i=1}^n \log \left[ \sum_{g=1}^G \pi_g \phi(\mathbf{x}_i \mid \boldsymbol{\mu}_g, \boldsymbol{\Sigma}_g) \right] \rightarrow \sum_{i=1}^n \sum_{g=1}^G z_{ig} \log \left[ \pi_g \phi(\mathbf{x}_i \mid \boldsymbol{\mu}_g, \boldsymbol{\Sigma}_g) \right] = l_{\mathcal{X}}$$

as the clusters separate. □

**Remark 4.** Although covariance matrices need only be positive semi-definite, we restrict  $\boldsymbol{\Sigma}$  to be positive definite in the proof of Lemma 1 so that  $\mathbf{X}$  is not degenerate.

## B.2 Proof of Parameter Estimate Convergence

Sample parameter estimates for the subset models converge to the parameter estimates for the full model. That is, as  $n_g \rightarrow \infty$ :

$$\begin{aligned}\hat{\pi}_{g \setminus j} &\rightarrow \hat{\pi}_g, \\ \bar{\mathbf{x}}_{g \setminus j} &\rightarrow \bar{\mathbf{x}}_g, \\ \mathbf{S}_{g \setminus j} &\rightarrow \mathbf{S}_g,\end{aligned}$$

where  $\hat{\pi}_g$ ,  $\bar{\mathbf{x}}_g$ , and  $\mathbf{S}_g$  are the sample proportion, mean, and covariance, respectively, for the  $g$ th cluster considering all observations in the entire dataset  $\mathcal{X}$ , and  $\hat{\pi}_{g \setminus j}$ ,  $\bar{\mathbf{x}}_{g \setminus j}$ , and  $\mathbf{S}_{g \setminus j}$  are the sample proportion, mean, and covariance, respectively, for the  $g$ th cluster considering only observations in the  $j$ th subset  $\mathcal{X} \setminus \mathbf{x}_j$ .

*Proof.* If  $z_{jh} = 1$ , then

$$\hat{\pi}_{h \setminus j} = \frac{n_h - 1}{n - 1}.$$

If  $z_{jh} = 0$ ,

$$\hat{\pi}_{h \setminus j} = \frac{n_h}{n - 1}.$$

Thus,

$$\hat{\pi}_{h \setminus j} \rightarrow \frac{n_h}{n} = \hat{\pi}_h$$

as  $n_h \rightarrow \infty$ . Now, for  $\bar{\mathbf{x}}_{h \setminus j}$  and  $\mathbf{S}_{h \setminus j}$ , if  $z_{jh} = 0$ , then  $\bar{\mathbf{x}}_{h \setminus j} = \bar{\mathbf{x}}_h$  and  $\mathbf{S}_{h \setminus j} = \mathbf{S}_h$  because

$$n_{h \setminus j} = n_h, \quad \bar{\mathbf{x}}_h = \frac{1}{n_h} \sum_{i=1}^n z_{ih} \mathbf{x}_i = \frac{1}{n_h} \sum_{i \neq j} z_{ih} \mathbf{x}_i = \bar{\mathbf{x}}_{h \setminus j},$$

$$\mathbf{S}_h = \frac{1}{n_h - 1} \sum_{i=1}^n z_{ih} (\mathbf{x}_i - \bar{\mathbf{x}}_h)(\mathbf{x}_i - \bar{\mathbf{x}}_h)' = \frac{1}{n_h - 1} \sum_{i \neq j} z_{ih} (\mathbf{x}_i - \bar{\mathbf{x}}_h)(\mathbf{x}_i - \bar{\mathbf{x}}_h)' = \mathbf{S}_{h \setminus j}.$$

If  $z_{jh} = 1$ ,

$$\bar{\mathbf{x}}_{h \setminus j} = \frac{n_h \bar{\mathbf{x}}_h - \mathbf{x}_j}{n_h - 1}.$$

Thus,  $\bar{\mathbf{x}}_{h \setminus j} \rightarrow \bar{\mathbf{x}}_h$  as  $n_h \rightarrow \infty$ . Therefore,  $\bar{\mathbf{x}}_{h \setminus j} \approx \bar{\mathbf{x}}_h$  and

$$\mathbf{S}_{h \setminus j} \approx \frac{1}{n_h - 2} [(n_h - 1)\mathbf{S}_h - (\mathbf{x}_j - \bar{\mathbf{x}}_h)(\mathbf{x}_j - \bar{\mathbf{x}}_h)'].$$

Thus,  $\mathbf{S}_{h \setminus j} \rightarrow \mathbf{S}_h$  as  $n_h \rightarrow \infty$ . □

## C Computation Time

Table 5 records the computation time in seconds for each algorithm. The entire OCLUST algorithm is timed without the p-value stopping criterion. The mean-shift algorithm is run in Python with 5000 random swaps. All other algorithms are run in R. Competing algorithms are run in series on a cluster with Intel Xeon Silver 4114 CPUs. The OCLUST algorithm was run on that same cluster for all datasets except Dim032. The benchmark and crabs datasets were run in parallel with 80 cores and the wine dataset was run with 20 cores. Dim032 was run with 30 cores on a separate cluster with Intel Xeon E5-4627 v2 CPUs.

Table 5: Computation time in seconds for each outlier identification algorithm on all datasets.

Dataset	(Full) OCLUST	Mean-Shift	2T	CNMix	NCM	DBSCAN
A1	5.43E+03	2.98E+04	2.38E+02	2.77E+02	6.14E+00	2.92E-01
A2	3.59E+04	6.42E+04	7.29E+02	1.44E+02	9.86E+00	2.46E-01
A3	1.21E+05	2.01E+05	2.11E+03	5.16E+03	3.71E+01	4.70E-01
S1	1.03E+04	4.28E+04	1.15E+02	1.84E+02	6.76E+00	2.69E-01
S2	1.75E+04	4.06E+04	2.14E+02	3.06E+02	1.03E+01	2.60E-01
S3	6.10E+04	3.13E+04	2.86E+02	3.50E+02	1.96E+01	3.07E-01
S4	1.27E+05	2.47E+04	3.60E+02	4.65E+02	2.19E+01	2.22E-01
Unbalance	9.33E+05	1.96E+04	3.80E+02	1.26E+02	5.53E+00	5.67E-01
Dim032	7.35E+03	8.566E+03	2.28E+02	1.55E+03	7.71E+01	3.05E-01
Wine	3.95E+02	1.80E+02	2.38E+02	5.62E+00	2.69E-01	7.09E-02
Crabs (avg.)	3.65E+00	1.06E+02	2.93E-02	9.02E-01	9.66E-02	3.66E-02